



# A strategic discovery roadmap towards high-quality leads and drug development candidates for kinetoplastid diseases. Part 2: from molecule to confirmed hit

Sarah Hendrickx<sup>1†</sup>, Kayhan Ilbeigi<sup>1†</sup>, Eli S.J. Thoré<sup>2,3</sup>, Michael G. Bertram<sup>2,4,5</sup>, Estefanía Calvo-Alvarez<sup>6</sup>, Sener Cintesun<sup>7</sup>, Ana Isabel Olías-Molero<sup>8</sup>, María Jesús Corral<sup>8</sup>, Marta Mateo-Barrientos<sup>9</sup>, Jérôme Estaquier<sup>10,11</sup>, Sébastien Pomel<sup>12</sup>, José María Alunda<sup>8</sup>, Sheraz Gul<sup>13,14</sup>, Katrien Van Bocxlaer <sup>15</sup>, Frédéric Frézard<sup>16</sup>, Joana Tavares<sup>17,18,19</sup>, Anabela Cordeiro Da Silva<sup>17,18,20</sup>, Maria Paola Costi<sup>21</sup>, Louis Maes<sup>1‡</sup> and Guy Caljon <sup>1\*‡</sup>

<sup>1</sup>Laboratory of Microbiology, Parasitology and Hygiene, University of Antwerp, Wilrijk (Antwerp) 2610, Belgium; <sup>2</sup>Department of Wildlife, Fish, and Environmental Studies, Swedish University of Agricultural Sciences, Umeå 907 36, Sweden; <sup>3</sup>Laboratory of Adaptive Biodynamics, Research Unit of Environmental and Evolutionary Biology, Institute of Life, Earth, and Environment, University of Namur, Namur 5000, Belgium; <sup>4</sup>Department of Zoology, Stockholm University, Stockholm 114 18, Sweden; <sup>5</sup>School of Biological Sciences, Monash University, Clayton Victoria 3800, Australia; <sup>6</sup>Department of Pharmacological and Biomolecular Sciences, University of Milan, Milan 20133, Italy; <sup>7</sup>Department of Molecular Biology and Genetics, Faculty of Arts & Science, Yildiz Technical University, Istanbul 34349, Turkey; <sup>8</sup>Department of Animal Health, Complutense University Madrid, Madrid 28040, Spain; <sup>9</sup>Department of Microbiology & Parasitology, Faculty of Pharmacy, Complutense University Madrid, Madrid 28040, Spain; <sup>10</sup>INSERM U1124, Université Paris Cité, Paris 75006, France; <sup>11</sup>Centre de Recherche du CHU de Québec, Université Laval, Québec, QC, G1V 4G2, Canada; <sup>12</sup>Université Paris-Saclay, CNRS BioCIS, 17 avenue des Sciences, Orsay 91400, France; <sup>13</sup>Fraunhofer Institute for Translational Medicine and Pharmacology ITMP, Discovery Research ScreeningPort, Hamburg 22525, Germany; <sup>14</sup>Fraunhofer Cluster of Excellence for Immune-Mediated Diseases CIMD, Hamburg 22525, Germany; <sup>15</sup>Skin Research Centre, Hull York Medical School, University of York, York YO10 5DD, UK; <sup>16</sup>Department of Physiology and Biophysics, Universidade Federal de Minas Gerais, Belo Horizonte, Minas Gerais 31270-901, Brazil; <sup>17</sup>i3S - Instituto de Investigação e Inovação em Saúde, Universidade do Porto, Porto 4200-135, Portugal; <sup>18</sup>IBMC - Instituto de Biologia Molecular e Celular, Universidade do Porto, Porto 4200-135, Portugal; <sup>19</sup>ICBAS - Instituto de Ciências Biomédicas Abel Salazar, Universidade do Porto, Porto 4200-135, Portugal; <sup>20</sup>Departamento de Ciências Biológicas, Faculdade de Farmácia da Universidade do Porto, Porto 4050-313, Portugal; <sup>21</sup>Department of Life Sciences, University of Modena and Reggio Emilia, Modena 41125, Italy

\*Corresponding author. E-mail: Guy.Caljon@uantwerpen.be

†Authors share first authorship.

‡Authors share senior authorship.

Given the medical importance and challenges related to kinetoplastid diseases, a strategic roadmap is needed for the identification of high-quality leads and drug development candidates. Within the aim to deliver more compelling proof-of-concept read-outs, this part proposes a systematic flow-chart of laboratory experiments and decision criteria, focusing on African trypanosomiasis, Chagas disease and visceral and cutaneous leishmaniasis. Next to precision experimental design and reporting, an overview is provided of various complementary laboratory models reproducing kinetoplastid infection and disease. Technical aspects of conventional *in vitro* and *in vivo* approaches and, more recently, *in silico* methods are presented with reference to specific pre-clinical R&D stages from ‘hit finding’ to ‘profiling of a confirmed hit’, covering the expertise areas of medicinal chemistry, primary pharmacology, (eco)toxicology, pharmacokinetics and pharmaceuticals (Figure 1).

## Medicinal chemistry: drug discovery in an era of computational methods

### Hit finding

The involvement of medicinal chemists is not only fundamental in the drug discovery process for the identification of active

compounds and new targets, but also for the initial production of small batches of compound and for the eventual scale-up of drug synthesis.

Hit finding generally starts from (i) the *in vitro* phenotypic evaluation of libraries of synthetic compounds, combinatorial chemistry or natural products against target organisms or (ii)

© The Author(s) 2026. Published by Oxford University Press on behalf of British Society for Antimicrobial Chemotherapy.

This is an Open Access article distributed under the terms of the Creative Commons Attribution-NonCommercial License (<https://creativecommons.org/licenses/by-nc/4.0/>), which permits non-commercial re-use, distribution, and reproduction in any medium, provided the original work is properly cited. For commercial re-use, please contact [reprints@oup.com](mailto:reprints@oup.com) for reprints and translation rights for reprints. All other permissions can be obtained through our RightsLink service via the Permissions link on the article page on our site—for further information please contact [journals.permissions@oup.com](mailto:journals.permissions@oup.com).

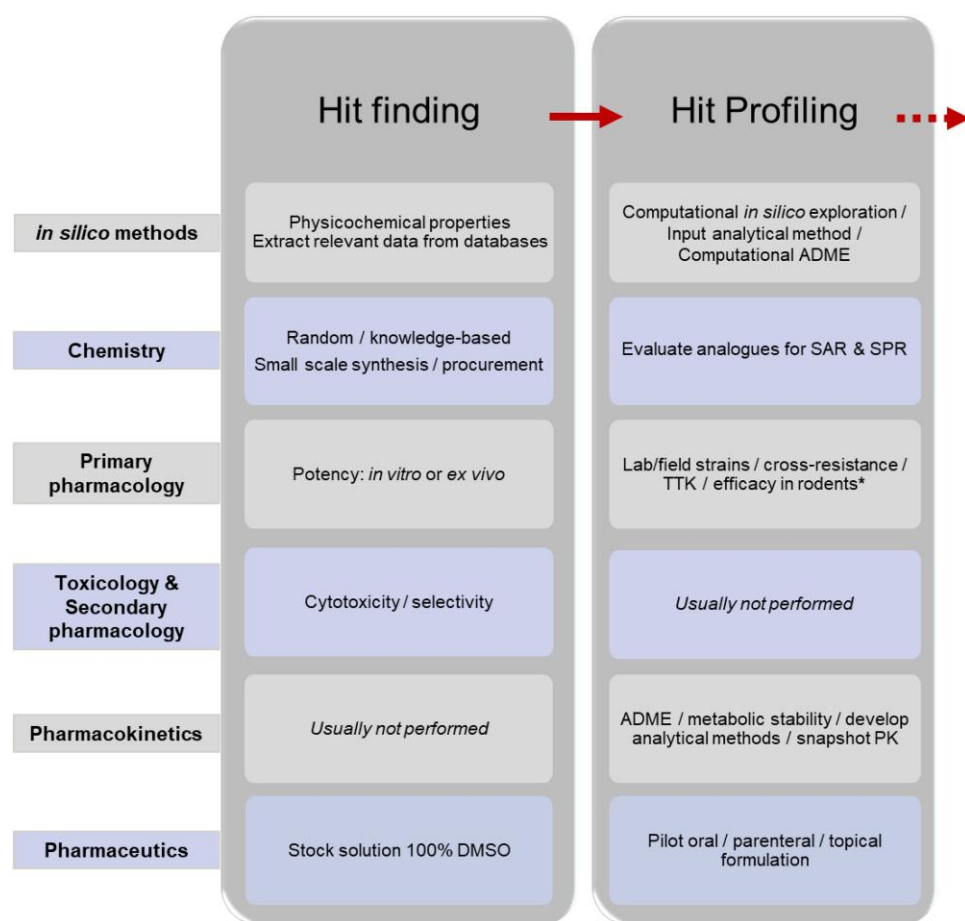


**Figure 1.** Schematic representation of the ‘baseline’ preclinical data package required during ‘hit finding’ and ‘hit profiling’, adopting a vertical (R&D stage) versus horizontal (discipline) tabular design. \* Conditional to a proper selectivity and PK profile. SPR, structure–property relationship.

knowledge-based approaches based on relevant targets, available ligands and virtual screening. Subsequently, biochemical assays can be developed that make use of the molecular target in isolation.<sup>1</sup> Alternatively, cell-based assays can be developed allowing detection of target activity directly by using a specific reporter or an entirely phenotypic approach.<sup>2,3</sup> Where the identity of a relevant protein is known, computational methods can now rapidly be adopted to identify compounds that bind and/or modulate their activities.<sup>4</sup> These approaches yield weakly active compounds, typically with potencies in the micromolar range, and do serve as chemical starting points for a drug.

The physicochemical properties of a chemical structure are key in determining its overall potential. For example, Lipinski’s Rule of Five may still be considered relevant as it provides a simple set of guides to assess drug-likeness and potential of oral bioavailability. By considering the molecular weight ( $\leq 500$  Daltons), lipophilicity ( $\log P \leq 5$ ), hydrogen bond donors ( $\leq 5$ ) and hydrogen bond acceptors ( $\leq 10$ ), research can be targeted to design new chemical entities (NCEs). Lipophilicity represents a main physicochemical characteristic that influences bioavailability, permeability and frequently also toxicity. The logarithm of the *n*-octanol partition coefficient ( $\log P$ ) is a basic predictor, while  $\log D$  was introduced as an improved descriptor for charged molecules at a

specific pH. Of particular interest is  $\log D_{7.4}$  which represents the partition coefficient using an aqueous phase buffered at physiological pH 7.4. A calculation tool for  $\log D$  has been developed using molecular signature descriptors and machine learning algorithms.<sup>5</sup> With the advent of high-quality curated databases relating to compounds such as DrugBank<sup>6</sup> and ChEMBL,<sup>7</sup> initial hit compounds for various targets can be identified with relative ease.

Another important aspect is the minimal quantity of compound required to perform assays at the *in vitro* stages of ‘hit finding’ and ‘hit profiling’ without the need for immediate re-synthesis. From a practical viewpoint, small-scale synthesis or procurement of about 5 mg should be sufficient, considering the synthesis efficiency and obtainable levels of purity. The assessment of purity of an initial synthesis batch is critical in relation to pharmacological outcome and should ideally reach  $>95\%$ . The analytical methodology includes a combination of chromatography, organic elemental microanalysis and quantitative NMR.<sup>8,9</sup>

The standard formulation of compounds for primary *in vitro* screening/evaluation is dissolution in 100% DMSO at 10 or 20 mM, while considering that the in-test concentration of DMSO should be  $\leq 1\%$ . Stock formulations can be stored at

room temperature, but utmost care should be taken to avoid water contamination since DMSO is highly hygroscopic whereby initial solutions can irreversibly turn into suspensions that are much less suited for further handling, dilution and testing.

### Hit profiling

Following the identification of a hit requires establishing a structure–activity relationship (SAR) with focus on understanding the role of chemical (sub)structures and the observed biological activity. The scaffold definition refers to the common essential chemical structure that can be substituted with different groups of various nature and dimension. The involvement of critical functional groups may significantly affect the biological potency and selectivity while reducing off-target effects. Linking structure and activity means to dissect the various molecular properties (electronic/steric environments and lipophilicity) that can explain why one compound in one homologous series is more active than others. The challenge in the hit profiling phase is to identify the most promising scaffold and associated modified compounds and ensure an understandable SAR description while maintaining a low micromolar biological activity. The toxicity profile is logically of utmost relevance whereby scaffolds of pan-assay interference compounds (PAINS) should be identified and excluded.<sup>10</sup>

The implementation of computational *in silico* methods allowing molecular docking of NCEs in putative target sites has strongly facilitated hit-to-lead optimization. Large datasets obtained from *in vitro* and *in vivo* studies have facilitated the prediction of physicochemical properties, SAR and ADMET (Absorption, Distribution, Metabolism, Excretion, and Toxicity) properties. QSAR studies are based on the assumption that similar chemicals will have similar physicochemical properties and toxicity. Software packages such as Flex X, GOLD, GLIDE, Autodock and Volsurf allow predicting docking potential into the putative active target site, PK parameters, associated toxicity and ecotoxicity early on in the discovery process.<sup>11</sup> The adverse outcome pathway (AOP) approach offers a framework for the risk assessment of chemicals providing knowledge to establish a relationship via key events (KEs) between a molecular initiating event and an adverse outcome in a biological setting.<sup>12</sup> Although *in silico* models are a simplistic representation of a system, they can be useful if applied within an AOP model description. More recently, the application of machine-learning-based concepts have evolved into the expansion of AI-driven discovery platforms.<sup>13</sup> Although some healthy scepticism and caution are still advisable when dealing with these computational tools, their application potential in drug discovery is vast and is expected to significantly reduce drug discovery timelines and cost.<sup>14,15</sup>

## Primary pharmacology: towards an integrated evaluation with focus on potency and selectivity

### Hit finding

Cell- and ‘whole organism’-based *in vitro* or *ex vivo* drug potency and selectivity

Compound activity must be evaluated against a well-characterized strain of the representative target species. *In vitro* methods remain the logical fundamental first step that allow

rapid, cost-effective, easy-to-perform and highly reproducible evaluations of a range of compounds avoiding premature involvement of laboratory animals.<sup>16</sup>

For extracellular trypanosomes, procyclic trypomastigote stages have frequently been used in the past for genetic engineering, but the bloodstream form remains the sole relevant life cycle stage for drug discovery purposes. Bloodstream forms of African trypanosome species (*Trypanosoma brucei gambiense*, *T. b. rhodesiense*, *T. b. brucei*, *T. b. evansi* type A, *T. b. equiperdum* and *T. congolense*) have been successfully adapted to axenic culture conditions by use of additives, such as methylcellulose or serum of specific host origin.<sup>17</sup> Bloodstream *T. b. brucei* stages are used as a safe surrogate for the human-infective subspecies *T. b. gambiense* and *T. b. rhodesiense*. Although efforts have been made to culture *T. vivax in vitro*,<sup>18</sup> an *ex vivo* setup is needed for drug susceptibility assays using bloodstream trypanosomes freshly isolated from infected donor mice.<sup>17,19,20</sup> Performing integrated *in vitro* and *ex vivo* assays for different trypanosome species with the ambition to select a pan-active compound is costly and time-consuming. Considering the phylogenetic differences between the various species,<sup>21</sup> initial testing against *T. b. brucei* followed by an evaluation against the phylogenetically most distinct *T. vivax* is a preferred and recently proven strategy as it facilitates the efficient selection of compounds likely to be effective across all HAT/AT species.<sup>17</sup> Susceptibility assays may slightly differ between species/strains and in *in vitro* and *ex vivo* settings, and are mostly related to the culture conditions, incubation time (48–120 h of drug exposure considering the *in vitro* survival time) and the number of parasites added per well (considering the proliferation rates). Endpoints are usually conducted with a metabolic read-out for cell viability, e.g. using resazurin<sup>22</sup> while new multiplexed biosensor assays are being developed.<sup>3</sup>

For the intracellular organisms *Leishmania* and *T. cruzi*, the choice of a suitable host cell was shown to influence drug susceptibility and ‘hit’ rate.<sup>23–25</sup> Various mammalian cell lines, such as mouse 3T3 and human MRC-5 fibroblasts,<sup>26–29</sup> rat L6 myoblasts<sup>25</sup> and monkey kidney epithelial Vero cells<sup>25</sup> are regularly used as host cells and for collecting *T. cruzi* trypomastigotes for a next round of infection. For *Leishmania* infections, different macrophage lines, mostly human such as THP-1<sup>30</sup> or murine such as J774 or RAW264.7,<sup>31</sup> are routinely used. A thorough comparison of different primary mouse macrophages already suggested the use of Swiss mouse-derived peritoneal exudate cells as an efficient, reliable, quick and cost-effective cell type.<sup>32</sup> Furthermore, infection of whole blood cells has provided another avenue for testing drug efficacy in primary human cells.<sup>33</sup> While the advantage of primary cells is their higher capacity to support infection and intracellular parasite multiplication, PMA-stimulated THP-1 cells represent a practical and animal-friendly alternative.<sup>24</sup> *Ex vivo* amastigotes, axenic amastigotes or stationary-phase promastigotes (rich in metacyclics) can be used for infection of cells. Spleen-derived amastigotes generally result in higher and more consistent infections but require the euthanasia of animals.<sup>24,34,35</sup> We strongly advise against the use of extracellular promastigote stages for drug screening purposes as stage-dependent differences in drug susceptibility have already been proved.<sup>36</sup> The comparison of activities against axenic and intramacrophage amastigotes can contribute to determine the

mode of action of the compound, e.g. its ability to cross membrane barriers in the macrophage, or its antileishmanial activity as a prodrug through host cell pathways.<sup>37</sup> As drug exposure influences efficacy on intracellular *Leishmania*,<sup>24</sup> the advice is to expose infected cells for 120 h during routine drug screening. Labour-intensive light microscopical analyses of the reduction in parasite loads compared with the non-treated controls are frequently used. Nowadays, more advanced quantitative techniques are available, such as bioluminescent/fluorescence assays using transgenic parasites, either or not in combination with advanced automated microscopic imaging and deep-learning algorithms.<sup>38-40</sup> These more advanced read-outs require high-content analysis platforms that are therefore not yet broadly implemented. Incorporating reference molecules into experimental assays is essential for accurately determining the relative potency of NCEs and for facilitating comparisons across different studies.

Selectivity should be considered from the very beginning of the drug discovery process using primary cell cultures and/or established cell lines.<sup>41</sup> Typical endpoints are based on biochemical, metabolism-based or cell membrane integrity-based parameters.<sup>42</sup>

### Hit profiling

#### *In vitro* cross-resistance and time-to-kill kinetics

Since all kinetoplastid-induced diseases face the emergence of drug resistance as a result of adaptive evolution,<sup>43</sup> early elimination of 'hits' compromised by cross-resistance against currently used drugs is warranted. Assessing efficacy against a wider panel of recent field or experimentally selected drug-resistant isolates can identify potential liabilities of cross-resistance. Furthermore, prioritizing compounds for *in vivo* follow-up may also benefit *in vitro* time-to-kill (TTK) studies<sup>44</sup> since incomplete killing may explain low efficacy or relapse. *In vitro* TTK studies are frequently used for AT to estimate the speed of cidal drug activity<sup>45,46</sup> as well as for *Leishmania* to evaluate concentration- and time-dependent cidal drug effects using the promastigote back-transformation assay to detect residual viable and growth-competent parasites.<sup>47,48</sup> Striking differences were noted between various antileishmanial reference drugs and novel Drugs for Neglected Diseases initiative drug leads, which strongly motivates for TTK inclusion in the pharmacodynamic profiling.<sup>47,48</sup>

#### Primary *in vivo* efficacy evaluation in laboratory rodent models

A recent literature review emphasized the poor consideration of animal welfare, human endpoint considerations, and the implementation of the 3Rs principle in antileishmanial drug discovery studies, and also highlighted the need to improve experimental study design in relation to statistical power.<sup>49</sup> Key factors that always need to be clearly defined are animal host species, host immune status, parasite strain and species, inoculation load and route of infection, measurement and analysis techniques, and defined endpoint criteria. Given these considerations, the UK Animals in Research Reporting *In Vivo* Experiments ARRIVE guidelines 2.0 and the ARRIVE Essential 10 (www.ARRIVEguidelines.org)<sup>50</sup> provide a useful framework including the Experimental Design Assistant (https://eda.nc3rs.org.uk).

**Table 1.** Overview of commonly used trypanosome strains to infect animal models

Disease	Parasite species	Parasite strains	References
Human African trypanosomiasis (HAT)	<i>T. b. rhodesiense</i>	STIB 900	45
		Etat1.2R	143
	<i>T. b. gambiense</i>	STIB 930	45
Animal trypanosomiasis (AT)	<i>T. b. brucei</i>	ITMAP141267	
		130R	
		45R	
		Squib 427	54
		EATRO 110	60
	<i>T. congolense</i>	AnTAR1	54
		TREU 667	60
		GVR 35/cl2	144
		CMP	56
		IL3000	145
	<i>T. vivax</i>	STIB 736/	146
		IL-1180	22
		TC13	
		STIB 719/ILRAD	146
		560	22
<i>T. b. evansi</i> type A	ILRAD700		
	STIB 806K	147	
	RoTat1.2	148	
	MCAM/ET/2013/004	149	
	MCAM/ET/2013/009	51	
<i>T. b. evansi</i> type B	Merzouga 93		
	MCAM/ET/2013/010	149	
	MCAM/ET/2013/014	150	
<i>T. b. equiperdum</i>	KETRI2479		
	BoTat	151,152	
	Dodola		
	OVI		
	TeAp-N/D1		

Similarly, the European Directorate for the Quality of Medicines and HealthCare (https://www.edqm.eu) provides support for 3Rs activities.

### Rodent models for human and animal trypanosomiasis

Considering the different diseases caused by HAT and AT species (Table 1), there is no ideal animal model that mimics the various parasite characteristics and disease manifestations. *T. b. brucei* is mostly used as a safe surrogate model for HAT given its close phylogenetic relationship with *T. b. rhodesiense* and *T. b. gambiense* and the shared characteristic of a tissue parasite that can cross the blood-brain barrier (BBB). For AT, several models using mouse-adapted strains of *T. congolense*, *T. vivax*, *T. b. evansi* and *T. b. equiperdum* have been established that can be used for primary drug testing to gain basic information on efficacy and safety at an early stage. Some of these infections reproduce the typical wasting disease observed in AT.<sup>51</sup>

Various inbred (C57BL/6, BALB/c, C3H/He, CBA) and outbred (Swiss Webster, NMRI) mouse strains are frequently used because they are cost-effective and can mimic both HAT and AT.<sup>52</sup> Reproducible infections in Swiss mice can be conveniently initiated for established AT strains by intraperitoneal (IP) inoculation of  $10^4$  parasites.<sup>17,53</sup> Swiss mice have been used in early- and late-stage models to evaluate drug efficacy both before and after CNS involvement.<sup>54</sup> Monomorphic infections such as those caused by *T. b. brucei* Lister 427 (Squib 427) involve non-variable single life stage parasites as mitotically dividing long slender forms.<sup>55</sup> Likewise, the *T. b. brucei* CMP strain proliferates rapidly in mice bloodstream and is lethal in <4 days.<sup>56</sup> These are typically used for early curative models since they do not mimic fluctuating parasitaemia and chronicity. In these models, treatment is initiated soon after (or sometimes before) infection and allows researchers to test the efficacy in the early stages of infection before the parasites have crossed the BBB.<sup>54,57</sup> Depending on the parasite species and strains, parasitaemia often reaches  $10^6$  parasites per mL of blood between 3 and 5 dpi, offering an ideal timeframe to initiate treatment under acute conditions. Pleomorphic infections, such as those caused by *T. b. brucei* TREU 927, AnTAR1/AnTat1.1 or GVR 35, involve parasites that can terminally differentiate to short-stumpy forms and demonstrate chronic infections similar to clinical cases.<sup>58,59</sup> These are used for late curative models with a CNS involvement, allowing for the evaluation of drug efficacy across the BBB. Treatment is initiated at about 3 weeks post-infection when parasites are known to have infiltrated the CNS and before animals start succumbing from infection. These models have successfully demonstrated the efficacy of compounds such as oxaboroles and nucleoside analogues in treating various stages of HAT.<sup>54,60</sup>

In all mouse models, parasitaemia levels are determined by counting parasites in peripheral blood. The use of bioluminescent models offers a valuable option of non-invasive *in vivo* imaging and longitudinal follow-up of the treatment in various tissues, including the brain. Pathology, primarily anaemia, is assessed in combination with the evolution of body weight typically within a 60-day post-treatment monitoring period. The endpoint for cure is recommended to involve determining the survival percentages and confirming the absence of viable parasite burdens by microscopy and molecular methods, such as a spliced-leader (SL) quantitative PCR (qPCR<sub>SL</sub> with reverse transcription, on target tissues (e.g. blood, spleen, brain)).<sup>61</sup> It is advisable to include at least a vehicle control, a reference drug-treated group and the test drug group under conditions of maximal (tolerable) drug exposure. A usual starting point is treatment at 50 mg/kg b.i.d. for five consecutive days. A standard added outcome includes measuring an *in vivo* dose–response relationship.

**Rodent models for Chagas disease** Specifically for Chagas disease, translation of promising ‘hits’ from *in vitro* to *in vivo* may more often fail by the inability to achieve complete parasite clearance. The intracellular amastigote form can infect any nucleated cell and has been found in cardiac tissue, adipose tissue, smooth muscle and the gastrointestinal tract.<sup>62–64</sup> Hence, a successful drug needs to effectively reach all sites of infection and eliminate parasites from these different locations. With regard to the latter, testing drugs for Chagas disease is more challenging, especially in the chronic phase of infection when it is hard

**Table 2.** Overview of commonly available strains to infect rodent models for Chagas disease

Disease	Parasite species	Parasite strains	References
Chagas disease acute and chronic phase	<i>T. cruzi</i>	Bioluminescent (red-shifted firefly luc) reporter clone CL-Brener	120
		Arequipa strain (MHOM/Pe/2011/Arequipa)	66
		Colombiana strain (benznidazole resistant)	68
Chagas disease acute phase	<i>T. cruzi</i>	Bioluminescent (firefly luc) line from Brazil heart-derived strain	117
		Bioluminescent or fluorescent (td-Tomato) expressing CL strain	119
		Bioluminescent (firefly luc) line from Y strain	118,153
		Tulahuen strain (TcVI) expressing the <i>E. coli</i> $\beta$ -galactosidase gene	69,71

to demonstrate sterile cure. During this phase, parasite burdens are extremely low, and tissue distribution is not well defined. Unlike in the acute phase where non-dividing trypomastigotes can be detected in the blood circulation by microscopy, parasitaemia in the chronic phase is mostly sub-patent. Murine models are for various reasons (cost, logistics, handling, application of new technologies) the most favoured and widely used to study infection and assess drug efficacy. They recapitulate many aspects of human disease, are easy to manipulate genetically and are amenable to BLI technologies.<sup>65</sup>

Mouse infections with *T. cruzi* classically include strains such as Arequipa,<sup>66</sup> Y strain,<sup>67,68</sup> Colombiana<sup>68</sup> and Tulahuen<sup>69</sup> (Table 2). Infections in BALB/c, A/J, Swiss, CH3 or C57BL/6 mice are usually initiated with intraperitoneal inoculation of *in vitro*-derived tissue-culture trypomastigotes ( $10^4$ ) or thawed cryopreserved bloodstream trypomastigotes ( $10^3$ – $10^5$ ). In the acute phase (4–15 dpi), parasite detection involves direct counting of trypomastigotes in the blood, while qPCR in various tissues is adopted during the chronic phase (75–120 dpi).<sup>66,67</sup> However, efficacy studies in the chronic phase with parasite detection using PCR and histology may be biased by the sampling procedure as parasites may hide in specific tissue depots.<sup>70</sup> Given the known parasite ‘persistence’ on chemotherapeutic treatment, mice are typically immunosuppressed with cyclophosphamide (200 mg/kg IP at 3–4 day intervals for a maximum of three doses) after the end of treatment to evaluate post-treatment relapse.<sup>71</sup>

Most murine studies have used traditional C57BL/6 mice that are relatively resistant to *T. cruzi* infection, making them an attractive model for chronic infection. Recently, a C57BL/6  $\alpha$ -1,3-galactosyltransferase knockout ( $\alpha$ -GalT-KO) mouse model has been described. As humans, these mice lack the  $\alpha$ -Gal trisaccharide epitope and are characterized by the massive production of infection-induced anti- $\alpha$ -Gal IgM and IgG. As a result, this

model closely resembles human disease where immunological resistance in chronic infections is correlated to the production of anti- $\alpha$ -Gal antibodies with concomitantly fewer parasite nests, lower parasitaemia and an increase of INF- $\gamma$ , TNF- $\alpha$  and IL-12 cytokines in the heart linked to cardiomyopathy.<sup>72</sup>

**Rodent models for leishmaniasis** As leishmaniasis is a family of related diseases with different clinical manifestations, several models have been described. While visceral leishmaniasis (VL) is typically caused by *L. donovani* and *L. infantum*, >15 species are aetiological agents of cutaneous leishmaniasis (CL). Mice and hamsters are the main species used in *in vivo* research, but the plethora of models make it difficult to extract a complete generalized protocol and to compare data across various laboratories.<sup>49</sup>

Despite several attempts to harmonize *in vitro* research,<sup>73–75</sup> fewer efforts have been made to standardize *in vivo* VL models.<sup>49,76–78</sup> In spite of the very detailed procedures described by Sacks and Melby in 2001,<sup>76</sup> many different animal models and procedures are still used. While the hamster model was well-accepted for VL infection studies until the 1980s,<sup>79</sup> mouse models now prevail to study host factors and immunology given their well-characterized genetic and immunological profiles. Also for CL, mice and hamsters are commonly used, each model's relevance depending on the research question, the *Leishmania* species under investigation and the aspect of the disease being studied. Mucocutaneous, diffuse cutaneous and PKDL models are currently still lacking and require a more comprehensive understanding of the host-pathogen interactions and drug susceptibilities.

**VL models** The development of a universal standardized VL mouse model is complicated by the difference in immune mechanisms associated with infection control in individual mouse strains. While BALB/c and C57BL/6 mice are known to be susceptible to VL, other strains (SV/129, DBA/2, C3H/He and Swiss) are considered to be naturally resistant.<sup>80</sup> Consistent with the importance of the adaptative immune responses,<sup>81</sup> immunodeficient Rag1- and Rag2-deficient mice are incapable of clearing parasites from the liver and are therefore sometimes used to cultivate virulent parasites *in vivo*.<sup>82,83</sup>

Most drug efficacy studies have used the BALB/c model since it has been most extensively immunologically characterized and shows a more susceptible phenotype to VL infection than C57BL/6 mice. A recommendation is to use six mice aged about 6–8 weeks per experimental group, in addition to a reference control and a placebo group.<sup>49</sup> Various *L. donovani* or *L. infantum* strains can be used, from well-characterized laboratory strains isolated in the 1960s to recent clinical isolates that might even be resistant to some currently used reference drugs (Table 3). Mice are infected with high doses ( $10^6$ – $10^8$ ) by either intravenous or IP injection, leading to visceral parasitism in spleen, liver and bone marrow. We recommend inoculation in the tail vein of highly virulent tissue-derived *ex vivo* (spleen-derived) amastigotes or low-passage stationary-stage promastigotes (*in vitro* passage <5) to ensure adequate and reproducible infectivity.<sup>84</sup> There is general consensus that parasites initially infect and multiply within the liver, followed by an immunological response and a delayed and persistent increase of splenic parasite burdens<sup>85–87</sup>

**Table 3.** Overview of a selection of major strains for *in vivo* leishmaniasis research

Disease	Parasite species	Parasite strains	References
VL	<i>L. infantum</i>	MHOM/MA/67/ITMAP-263	154
		MHOM/FR/96/LEM3323	89
		MCAN/ES/96/BCN150	155
	<i>L. donovani</i>	LV9 (MHOM/ET/67/HU3)	156,157
		LV82	158
CL	<i>L. major</i>	Friedlin	159
		LV39c5 (RHO/SU/59/P)	157
		JISH118 (MHOM/SA/85/JISH118)	106
	<i>L. amazonensis</i>	MHOM/BR/77/LTB0016	160
		MHOM/BR/75/Josefa	161
		MPRO/BR/72/M1845, LV78	161
	<i>L. braziliensis</i>	MHOM/BR/94/H3227	162

in which the immunosuppressive IL-10 is associated with disease progression.<sup>88</sup> Some studies indicate early involvement of the bone marrow while others report bone marrow involvement in more progressive phases of disease.<sup>89,90</sup> This typical pattern of spontaneous parasite clearance in mice highlights the need to carefully reflect on the timing of drug administration. A recent study proposed waiting until 21 days post-infection before initiating treatment,<sup>49</sup> whereas others favour a start of treatment 7 days post-infection and autopsy 5 days after the last treatment dose to provide a better assay window.<sup>89</sup> Autopsy is performed to collect tissue samples for microscopic quantification of residual parasite burdens in Giemsa-stained tissue imprints, limiting dilution assays and PCR.

While progression of *Leishmania* infection in hamsters is considered to more closely reflect the pathology of human VL,<sup>91,92</sup> applicability of such models is limited because of ethical objections (larger animal species, lack of easily accessible veins), lack of immunological and genetic tools and the higher costs of animal housing.<sup>93</sup> Most commonly used is the Syrian or golden hamster (*Mesocricetus auratus*) since this species presents a similar VL pathology to that of humans with hepatosplenomegaly, ascites, weight loss, cachexia, pancytopenia, hypergammaglobulinemia and death if left untreated. The Syrian hamster model is also valid to evaluate drug efficacy in a progressive infection after inoculation of doses ranging from  $10^6$ – $10^8$  parasites. Infection of six hamsters per group (6–8 weeks old) with a dose of  $2 \times 10^7$  *ex vivo* spleen-derived amastigotes is recommended. Intracardial (IC) injection is a highly effective administration route but requires highly skilled personnel and raises ethical concerns, for which retro-orbital inoculation can serve as an alternative.<sup>94</sup> For early curative evaluation, a 5- to 10-day treatment regimen typically starts at 21 days after infection, i.e. before the appearance of lesions or signs. For the late curative evaluation, treatment is delayed until 42 days post-infection, i.e. when the infection is already advanced. Autopsy is commonly performed 10 days after the end of treatment (at day 35 or day 56 post-infection) for quantification of visceral parasite loads, using tissue imprints, limiting dilution assays and molecular methods.<sup>93</sup> The

use of automated imaging/counting software can exclude a more subjective interpretation by non-experts while a standardized PCR read-out is recognized as the most objective quantification system.<sup>49</sup> Several PCR methods have been proposed over the years, mostly targeting the minicircle kinetoplast DNA, which is less suited for drug discovery research as it requires adaptation of the primers for the various *Leishmania* species, and it reflects less the dynamic effects of treatment on viable parasite burdens. A comprehensive comparison of various real-time PCR assays in tissue and blood samples of animals and human patients demonstrated excellent analytical sensitivity of a new pan-*Leishmania* RNA real-time qPCR assay targeting the conserved and highly expressed SL mini-exon sequence in viable parasites.<sup>95,96</sup>

**CL models** Inbred BALB/c and C57BL/6 mice are the two most common mouse strains in CL research. BALB/c mice are highly susceptible and manifest severe non-healing often ulcerating lesions that progress rapidly<sup>97</sup> involving compromised function of T-cells, macrophages or both.<sup>98</sup> In contrast, C57BL/6 mice exhibit greater resistance to *L. major* and *L. amazonensis*, effectively controlling the infection and limiting lesion development. The distinct responses between BALB/c and C57BL/6 mice underscore the importance of host genetics in disease outcome and provide a comparative framework for investigating immune mechanisms. Given their inability to raise a protective immune response, BALB/c mice are more often used in drug efficacy studies. Next to genetic differences in CL susceptibility, sex-determined differences can potentially affect CL progression.<sup>99</sup> Golden hamsters also serve as important model for CL, in particular for those strains that demonstrate low infectivity to mice, such as the subgenus *Viannia* species closely mimicking human pathology with chronic lesions that often metastasize either in the skin or to mucosal tissues.

Contrary to VL models in which amastigote forms are mostly used to initiate reproducible infections, for CL infective stationary-phase promastigotes selected with peanut agglutinin<sup>100</sup> or density gradient centrifugation<sup>101</sup> are generally injected intradermally (ID) or subcutaneously (SC).<sup>102,103</sup> Although a sand fly bite deposits ~10 to 100 000 parasites in the skin in natural infections,<sup>104,105</sup> models investigating drug efficacy often use higher parasite loads (~10<sup>5</sup>–10<sup>7</sup>) to establish a reproducible model with consistent lesion development across test subjects.<sup>106,107</sup> This approach is based on direct correlation between the number of parasites and lesion size development as a measure of disease severity.<sup>108,109</sup>

Different inoculation sites may influence clinical manifestations, disease progression and immune responses.<sup>110</sup> The ear is often favoured due to its accessibility and ease of monitoring lesion development, although it misses the subdermal layer. By contrast, the rump and footpad provide a more comprehensive representation of human skin anatomy, facilitating the collection of larger tissue samples for detailed histopathological and molecular analyses. Hindrance of mouse movement following footpad injections raises ethical considerations, hence requiring careful monitoring and management of animal welfare during experimental procedures.

Disease progression and impact of treatment can be evaluated by non-invasive measurement of the lesion size using

(digital) callipers. In this simple and widely used method, the diameter (in two perpendicular directions) and thickness of lesions are measured. Histopathological analysis of tissue sections can also be examined to assess the extent of cellular infiltration, tissue damage and parasite burden. As an endpoint measurement, tests of cure can be based on quantitative PCR for *Leishmania* kinetoplast DNA or spliced leader (SL)-RNA, or by limiting dilution assays involving culturing serial dilutions of tissue homogenates to estimate the number of viable parasites.

**Bioluminescence imaging: a versatile tool to monitor drug kinetics and identify parasite niches** For monitoring parasite burdens over time, *in vivo* imaging using either bioluminescence (BLI) or fluorescence are proposed as more refined methods.<sup>49</sup> The construction of bioluminescent parasites and the application of *in vivo* imaging offers a valuable and sensitive alternative allowing longitudinal follow-up of the same animal during drug exposure and treatment relapse hereby uncovering potential parasite niches.<sup>111</sup> The number of animals can be reduced to 3–5 animals per group when the infecting strain is sufficiently characterized. When the limit of detection is adequate, BLI can uncover sites in the body that are pharmacokinetically unfavourable and cannot sufficiently be reached by drugs, or sanctuary sites where parasites can reside in a quiescent state. Both may lead to treatment failure and/or post-treatment relapse, which are important caveats in drug R&D.

BLI has uncovered how *T. brucei* colonizes various host tissues beyond the bloodstream and the CNS. In addition to the skin and adipose tissue,<sup>112,113</sup> the lungs and pancreas emerged as other parasite reservoirs.<sup>114,115</sup> This new understanding of tissue tropisms and extravascular dissemination not only challenges the traditional focus on bloodstream parasites but also highlights the need for targeted interventions that address these hidden reservoirs to effectively control and eliminate AT.

BLI was also shown to be a validated, highly sensitive technique for monitoring *T. cruzi* infections. The most sensitive model uses BALB/c mice infected with a transgenic CL-Brener *T. cruzi* expressing a red-shifted luciferase that emits light in the tissue-penetrating orange-red region of the spectrum.<sup>111,116</sup> Other mouse models are mainly used for acute disease and include infections with BLI strains derived from the Brazil heart-derived strain<sup>117</sup> and Y strain,<sup>118</sup> and fluorescent or bioluminescent lines derived from the CL-Brener strain.<sup>119</sup> Efficacy studies at the chronic phase involve drug treatments ranging between 74 and 127 days post-infection.<sup>120,121</sup> The limit of detection in live animals is <10<sup>3</sup> parasites and endpoint *ex vivo* BLI allows tissue-specific quantification of parasite loads in individual mice with minimal sampling bias.<sup>111,120</sup> Cyclophosphamide-induced immunosuppression enhances the detection of relapses using *ex vivo* imaging of individual organs/tissues at the experiment endpoint<sup>120</sup> and identified the gut as a parasite reservoir in the chronic phase.<sup>111</sup>

BLI has also evolved as a useful tool to follow-up *Leishmania* infections in both mice<sup>84,89,90,122</sup> and Syrian golden hamsters<sup>123</sup> with a limit of detection of ~10<sup>6</sup> parasites or higher in the viscera<sup>89,90</sup> and ~10<sup>4</sup> in skin.<sup>124,125</sup> This detection limit is relatively high compared with the available molecular methods and forces researchers to increase the inoculum size to 10<sup>8</sup>–10<sup>9</sup> metacyclic

promastigotes or axenic amastigotes per mouse.<sup>90,122,126</sup> Variations in the kinetics of tissue colonization are apparent from BLI models in different laboratories due in part to the use of different strains. Observations varied between the apparent absence of detectable infection<sup>93</sup> to early (coinciding with the liver peak<sup>89</sup>) or late infection (coinciding with the spleen peak<sup>90</sup>) of the bone marrow. Infection of BALB/c mice with *L. donovani* even revealed a spleen peak as early as 7 dpi<sup>84</sup> while the spleen is generally colonized only in progressed infections. Longitudinal follow-up does not only allow assessment of cidal drug kinetics but can also detect parasite niches and potential sources of post-treatment relapse.<sup>122,126</sup> These studies recently pinpointed stem cells in the bone marrow as a specific 'immunomicrotope' or sanctuary niche for post-treatment relapse<sup>126,127</sup> in which *Leishmania* parasites acquire a quiescent phenotype that is more resilient to drug action.<sup>128</sup>

## Toxicology: need for early assessment of go/no-go criteria

### Hit finding

Selectivity is of primary importance from the very beginning of the drug discovery process. Cytotoxicity/selectivity testing is preferably performed on suitable primary cell cultures and/or established cell lines. Although primary cells are biologically more relevant, they may be less suitable for large-scale comprehensive screens as the number of cells that can be obtained from a given tissue is limited. As such, *in vitro* cytotoxicity is mostly evaluated on immortalized cell lines<sup>41</sup> using biochemical, metabolism-based or cell membrane integrity-based endpoints.<sup>42</sup> For example, a recent review of cytotoxicity studies for antileishmanial drugs showed that most studies used MTT (66%), followed by Alamar Blue (17%) and Trypan Blue (4.5%).<sup>129</sup> Recent endeavours in robotic assay design have helped to accommodate high throughput screening using a minute amount of compound.<sup>130</sup> Recent studies using primary human cells have established the potential side effects of drugs related to immune cell proliferation, mitochondria damage and cell death including the activation of the inflammasome in innate immune cells.<sup>131</sup> Besides the cytotoxicity/selectivity assessment, intrinsic toxicity characteristics are not yet considered at the hit finding stage, partly due to the limited availability of compound. Important factors in the *in vitro* cytotoxicity evaluation are the choice of cell type (primary versus continuous), confluent versus non-confluent, serum content in the culture medium, duration of cell exposure and type of endpoint. In general, CC<sub>50</sub> values below 10 μM may tend to become problematic and should trigger a more critical view on selectivity of action and toxicity issues later in development.<sup>16,132</sup>

### Hit profiling

The first evaluation in laboratory rodent models of confirmed *in vitro* hits should preferentially adopt conditions of high (oral) drug exposure, not only to primarily discern discrete signs of putative pharmacological activity potential, but also for early signs of intolerance. Depending on the disease model, a treatment regimen using high doses (e.g. 50 mg/kg b.i.d) for several

consecutive days (≥5 days) needs to be considered. The modified Irwin procedure or functional observational battery can serve as a complementary procedure to detect gross functional and neurobehavioral deficits related to compound exposure.<sup>130,133</sup> Signs of intolerance or toxicity include body weight loss (>10%), rough haircoat, changed behaviour and even mortality, hence necessitating explorative dose-titration experiments.

## Pharmacokinetics: aiming for oral bioavailability and distribution to target tissues

### Hit profiling

Although potency and selectivity of confirmed *in vitro* hits are the essential starting point, *in vivo* activity will largely be determined by the compound absorption, distribution, metabolism, excretion (ADME) properties that are not captured in the initial phenotypic assays for potency. Indeed, problems with the ADME processes cause many 'hits' with a promising *in vitro* activity profile to fail *in vivo*. However, a stringent selection and fast attrition based on computational ADME studies and realistic criteria *in vitro* can already reduce the need for animal studies. SAR and structure-property relationship analyses will support lead candidate identification and further lead optimization to improve the pharmacokinetic properties. The pharmacokinetics are largely determined by the compound's physicochemical properties that affect oral bioavailability, distribution to relevant target organs, metabolic stability and renal clearance, all determining the compound's systemic exposure and half-life. Several *in vitro* assays exist to assess absorption (e.g. Caco-2 cells) and metabolism (microsomes) and help identifying the best candidates to move forward for subsequent *in vivo* evaluation. As explained later, formulation can also further improve bioavailability depending on the application.

For absorption, *in vitro* assays endorsed by the EMA and the FDA are in place using monolayers of human colonic adenocarcinoma Caco-2 cells to evaluate the compound's transcellular permeation.<sup>134</sup> This Caco-2 system has the benefit over the parallel artificial membrane permeability assay in that it expresses many structural and functional characteristics of human enterocytes, including the expression of influx and efflux transporters and several digestive enzymes. The integrity of the Caco-2 cell monolayer before and after the permeation assay is essential for the validity of the assay and is assessed with trans-epithelial electrical resistance measurements (>300 Ω×cm<sup>2</sup>).<sup>135</sup> Moreover, model drugs with known human intestinal absorption need to be included as comparators within the categories of high-, moderate-, low- and zero-permeability compounds and efflux substrates.<sup>134</sup> Experimental permeation data are expressed as apparent permeability coefficient values ( $P_{app}$ ; high-permeability: >10×10<sup>-6</sup> cm/s, moderate-permeability: 1–10×10<sup>-6</sup> cm/s) and provide, together with the aqueous solubility, a basis for predicting whether a compound can be administered orally.

First-pass effects that result in orally administered compounds undergoing metabolic degradation have a large impact on obtaining systemic therapeutic concentrations. The liver is

considered as a major site where first-pass metabolism occurs, although other tissues can participate in this process as well.<sup>136,137</sup> The *in vitro* metabolic stability should preferably be determined at an early stage to anticipate the possibility of *in vivo* biotransformation by modifying enzymes of the liver, i.e. the cytochrome P450 (CYP) superfamily (Phase-I metabolism) and glucuronosyl- and acetyltransferase enzymes (Phase-II metabolism). Commercially available liver microsomal S9 fractions from toxicology (mouse, rat, dog) and target species allow a relatively straightforward comparative assessment of the metabolic stability of the parent compound on addition of the co-factors, such as reduced NADPH or uridine diphosphate glucuronic acid to detect Phase-I or -II metabolization. If parent compound clearance is >50% within 30 minutes, compounds are considered metabolically unstable. To note is that microsomes of rodent species often have higher metabolizing activities than those of target species. The inclusion of a non-selective cytochrome inhibitor, 1-aminobenzotriazole (1-ABT), inhibits Phase-I metabolism and often prevents decay in the microsomal stability test. 1-ABT can later also be applied in downstream animal studies to circumvent underestimation of compound potency in high-metabolizing animal models.

The logistic limitation of the inclusion of these assays is the need for HPLC and MS bioanalytical methods to quantify the parent compound and ideally also the resulting major metabolites. As an alternative, researchers might reside to *in silico* prediction of the metabolic stability of identified hit compounds using the novel computational deep-learning modelling tool 'Systems Metabolomics using Interpretable Learning and Evolution' (SMILE),<sup>138</sup> although the results should be interpreted with caution.

The first exploratory small-scale *in vivo* efficacy studies (*vide supra*) could be preceded by a snapshot PK study<sup>139</sup> using a minimal number of mice ( $n=2$ ) and compound (starting from a 3–5 mg batch) and considering a limited number of sampling time points (0.5, 1, 3 and 5 h post-dosing) and small blood volumes (50  $\mu$ L) for reason of animal welfare. Repeated blood sampling from mice is generally performed using the tail vein and is worldwide considered ethically justified if not >10% of the total blood volume is removed on a single occasion every three to four weeks.<sup>140</sup> Alternative serial sampling techniques use the retro-orbital or lateral saphenous vein puncture.<sup>141</sup> In case repeated blood samples are required at short intervals, a maximum of 0.6 mL/kg/day or 1.0% of an animal's total blood volume can be removed every 24 h.<sup>140</sup> The collection of dried blood spots onto FTA<sup>®</sup> DMPK-cards is very convenient as it is compatible with small sampling volumes, inactivation of the parasitic organisms, convenient storage and transport. The same analytical methods as in the *in vitro* profiling are used for the quantification of parent compound in dried blood spot/plasma, and non-compartmental PK regression analysis allows calculation of typical standard output parameters such as the AUC (area under the plasma concentration time curve), Cl (clearance),  $V_{ss}$  (volume of distribution at steady-state),  $T_{1/2}$  (half-life of elimination),  $C_{max}$  (maximum plasma concentration) and  $T_{max}$  (time at which  $C_{max}$  occurs). Compounds with moderate and high exposure based on their AUC and plasma concentration profile can then be prioritized for a more extended evaluation.

## Pharmaceutics

### Hit profiling

At the stage of the hit profiling, compound resources are still limited precluding extensive exploratory formulation work. However, to accommodate the first *in vivo* efficacy evaluation in laboratory rodents, rescue for moderate/poorly aqueous soluble compounds can be taken by using several standard vehicles for making oral (e.g. 1% hydroxypropyl methylcellulose, 100% PEG 400 or 5% Tween 80), topical (e.g. 1% hydroxyethyl cellulose hydrogel, containing or not propylene glycol) or parenteral (e.g. 20% PEG 400, 5% DMSO or 0.5% Tween 80) pilot formulations. An overview of excipients/vehicles and tolerable levels through various routes of administration in multiple species based on a rigorous data mining operation is presented in a comprehensive review.<sup>142</sup>

### Acknowledgements

This article is based on work from COST Action OneHealthdrugs (CA21111). LMPH is a partner of the Excellence Centre 'Infla-Med' ([www.uantwerpen.be/infla-med](http://www.uantwerpen.be/infla-med)).

### Funding

This work is supported by COST Action OneHealthdrugs (CA21111). The Action is supported by COST (European Cooperation in Science and Technology). G.C. is supported by the Fonds Wetenschappelijk Onderzoek (FWO) Vlaanderen (G065421N and G0A5624N). M.G.B. was supported by the Swedish Research Council Formas (2020-02293) and the Kempe Foundation (SMK-1954 and SMK21-0069).

### Transparency declarations

None to declare.

### References

- Zhou Y, Zhang Y, Zhao D *et al.* TTD: Therapeutic Target Database describing target druggability information. *Nucleic Acids Res* 2024; **52**: D1465–D77. <https://doi.org/10.1093/nar/gkad751>
- Moffat JG, Rudolph J, Bailey D. Phenotypic screening in cancer drug discovery—past, present and future. *Nat Rev Drug Discov* 2014; **13**: 588–602. <https://doi.org/10.1038/nrd4366>
- Call DH, Adjei JA, Pilgrim R *et al.* A multiplexed high throughput screening assay using flow cytometry identifies glycolytic molecular probes in bloodstream form *Trypanosoma brucei*. *Int J Parasitol Drugs Drug Resist* 2024; **26**: 100557. <https://doi.org/10.1016/j.ijpddr.2024.100557>
- Sadybekov AV, Katritch V. Computational approaches streamlining drug discovery. *Nature* 2023; **616**: 673–85. <https://doi.org/10.1038/s41586-023-05905-z>
- Wang Y, Xiong J, Xiao F *et al.* Logd7.4 prediction enhanced by transferring knowledge from chromatographic retention time, microscopic  $pK_a$  and logP. *J Cheminform* 2023; **15**: 76. <https://doi.org/10.1186/s13321-023-00754-4>
- Knox C, Wilson M, Klinger CM *et al.* DrugBank 6.0: the DrugBank Knowledgebase for 2024. *Nucleic Acids Res* 2024; **52**: D1265–D75. <https://doi.org/10.1093/nar/gkad976>
- Zdrazil B, Felix E, Hunter F *et al.* The ChEMBL Database in 2023: a drug discovery platform spanning multiple bioactivity data types and time

- periods. *Nucleic Acids Res* 2024; **52**: D1180–D92. <https://doi.org/10.1093/nar/gkad1004>
- 8** Pauli GF, Chen SN, Simmler C *et al.* Importance of purity evaluation and the potential of quantitative  $^1\text{H}$  NMR as a purity assay. *J Med Chem* 2014; **57**: 9220–31. <https://doi.org/10.1021/jm500734a>
- 9** Kandoller W, Theiner J, Keppler B *et al.* Elemental analysis: an important purity control but prone to manipulations. *Inorg Chem Front* 2022; **9**: 412–6. <https://doi.org/10.1039/D1QI01379C>
- 10** Baell JB, Holloway GA. New substructure filters for removal of pan assay interference compounds (PAINS) from screening libraries and for their exclusion in bioassays. *J Med Chem* 2010; **53**: 2719–40. <https://doi.org/10.1021/jm901137j>
- 11** Masimirembwa C, Thelingwani R. Application of in silico, in vitro and in vivo ADMET/PK platforms in drug discovery. In: Chibale K, Davies-Coleman M, Masimirembwa C, eds. *Drug Discovery in Africa: Impacts of Genomics, Natural Products, Traditional Medicines, Insights into Medicinal Chemistry, and Technology Platforms in Pursuit of New Drugs*. Springer, 2012; 151–91.
- 12** Halappanavar S, van den Brule S, Nyman P *et al.* Adverse outcome pathways as a tool for the design of testing strategies to support the safety assessment of emerging advanced materials at the nanoscale. *Part Fibre Toxicol* 2020; **17**: 16. <https://doi.org/10.1186/s12989-020-00344-4>
- 13** Atomwise AIMS Program. Author Correction: AI is a viable alternative to high throughput screening: a 318-target study. *Sci Rep* 2024; **14**: 21579. <https://doi.org/10.1038/s41598-024-70321-w>
- 14** Vijayan RSK, Kihlberg J, Cross JB *et al.* Enhancing preclinical drug discovery with artificial intelligence. *Drug Discov Today* 2022; **27**: 967–84. <https://doi.org/10.1016/j.drudis.2021.11.023>
- 15** Balatti GE, Barletta PG, Perez AD *et al.* Machine learning approaches to improve prediction of target-drug interactions. In: *Drug Design Using Machine Learning*. Wiley, 2022; 21–96. <https://doi.org/10.1002/9781394167258.ch2>
- 16** Hendrickx S, Caljon G, Maes L. *In vitro* growth inhibition assays of *Leishmania* spp. *Methods Mol Biol* 2020; **2116**: 791–800. [https://doi.org/10.1007/978-1-0716-0294-2\\_47](https://doi.org/10.1007/978-1-0716-0294-2_47)
- 17** Ilbeigi K, Mabile D, Matheussen A *et al.* Discovery and development of an advanced lead for the treatment of African trypanosomiasis. *ACS Infect Dis* 2025; **11**: 131–43. <https://doi.org/10.1021/acsinfecdis.4c00472>
- 18** D'Archivio S, Medina M, Cosson A *et al.* Genetic engineering of *Trypanosoma (Duttonella) vivax* and in vitro differentiation under axenic conditions. *PLoS Negl Trop Dis* 2011; **5**: e1461. <https://doi.org/10.1371/journal.pntd.0001461>
- 19** Lanham SM, Godfrey DG. Isolation of salivarian trypanosomes from man and other mammals using DEAE-cellulose. *Exp Parasitol* 1970; **28**: 521–34. [https://doi.org/10.1016/0014-4894\(70\)90120-7](https://doi.org/10.1016/0014-4894(70)90120-7)
- 20** Gutierrez C, Corbera JA, Doreste F *et al.* Use of the miniature anion exchange centrifugation technique to isolate *Trypanosoma evansi* from goats. *Ann N Y Acad Sci* 2004; **1026**: 149–51. <https://doi.org/10.1196/annals.1307.020>
- 21** Stevens JR, Gibson WC. The evolution of pathogenic trypanosomes. *Cad Saude Publica* 1999; **15**: 673–84. <https://doi.org/10.1590/S0102-311X1999000400002>
- 22** Mabile D, Ilbeigi K, Hendrickx S *et al.* Nucleoside analogues for the treatment of animal trypanosomiasis. *Int J Parasitol Drugs Drug Resist* 2022; **19**: 21–30. <https://doi.org/10.1016/j.ijpddr.2022.05.001>
- 23** Seifert K, Escobar P, Croft SL. In vitro activity of anti-leishmanial drugs against *Leishmania donovani* is host cell dependent. *J Antimicrob Chemother* 2010; **65**: 508–11. <https://doi.org/10.1093/jac/dkp500>
- 24** Hendrickx S, Van Bockstal L, Caljon G *et al.* In-depth comparison of cell-based methodological approaches to determine drug susceptibility of visceral *Leishmania* isolates. *PLoS Negl Trop Dis* 2019; **13**: e0007885. <https://doi.org/10.1371/journal.pntd.0007885>
- 25** Franco CH, Alcântara LM, Chatelain E *et al.* Drug discovery for Chagas disease: impact of different host cell lines on assay performance and hit compound selection. *Trop Med Infect Dis* 2019; **4**: 82. <https://doi.org/10.3390/tropicalmed4020082>
- 26** Guimarães-Pinto K, Nascimento DO, Corrêa-Ferreira A *et al.* *Trypanosoma cruzi* infection induces cellular stress response and senescence-like phenotype in murine fibroblasts. *Front Immunol* 2018; **9**: 1569. <https://doi.org/10.3389/fimmu.2018.01569>
- 27** Martínez-Peinado N, Cortes-Serra N, Sherman J *et al.* Identification of *Trypanosoma cruzi* growth inhibitors with activity in vivo within a collection of licensed drugs. *Microorganisms* 2021; **9**: 406. <https://doi.org/10.3390/microorganisms9020406>
- 28** Sykes ML, Avery VM. Development and application of a sensitive, phenotypic, high-throughput image-based assay to identify compound activity against *Trypanosoma cruzi* amastigotes. *Int J Parasitol Drugs Drug Resist* 2015; **5**: 215–28. <https://doi.org/10.1016/j.ijpddr.2015.10.001>
- 29** de Araújo JS, García-Rubia A, Sebastián-Pérez V *et al.* Imidazole derivatives as promising agents for the treatment of Chagas disease. *Antimicrob Agents Chemother* 2019; **63**: e02156–18. <https://doi.org/10.1128/AAC.02156-18>
- 30** Das N, Roy J, Patra B *et al.* Hit-to-lead optimization of 2-aminoquinazolines as anti-microbial agents against *Leishmania donovani*. *Eur J Med Chem* 2024; **269**: 116256. <https://doi.org/10.1016/j.ejmech.2024.116256>
- 31** Pomel S, Cojean S, Pons V *et al.* An adamantamine derivative as a drug candidate for the treatment of visceral leishmaniasis. *J Antimicrob Chemother* 2021; **76**: 2640–50. <https://doi.org/10.1093/jac/dkab226>
- 32** Van den Kerkhof M, Bockstal V, Gielis L *et al.* Impact of primary mouse macrophage cell types on *Leishmania* infection and in vitro drug susceptibility. *Parasitol Res* 2018; **117**: 3601–12. <https://doi.org/10.1007/s00436-018-6059-4>
- 33** Picard M, Soundaramourty C, Silvestre R *et al.* *Leishmania infantum* infection of primary human myeloid cells. *Microorganisms* 2022; **10**: 1243. <https://doi.org/10.3390/microorganisms10061243>
- 34** Mendes Costa D, Cecilio P, Santarém N *et al.* Murine infection with bioluminescent *Leishmania infantum* axenic amastigotes applied to drug discovery. *Sci Rep* 2019; **9**: 18989. <https://doi.org/10.1038/s41598-019-55474-3>
- 35** da Luz RI, Vermeersch M, Dujardin JC *et al.* *In vitro* sensitivity testing of *Leishmania* clinical field isolates: preconditioning of promastigotes enhances infectivity for macrophage host cells. *Antimicrob Agents Chemother* 2009; **53**: 5197–203. <https://doi.org/10.1128/AAC.00866-09>
- 36** Vermeersch M, da Luz RI, Tote K *et al.* *In vitro* susceptibilities of *Leishmania donovani* promastigote and amastigote stages to antileishmanial reference drugs: practical relevance of stage-specific differences. *Antimicrob Agents Chemother* 2009; **53**: 3855–9. <https://doi.org/10.1128/AAC.00548-09>
- 37** Obeid S, Berbel-Manaia E, Nicolas V *et al.* Deciphering the mechanism of action of VP343, an antileishmanial drug candidate, in *Leishmania infantum*. *iScience* 2023; **26**: 108144. <https://doi.org/10.1016/j.isci.2023.108144>
- 38** Juez-Castillo G, Valencia-Vidal B, Orrego LM *et al.* FiCRoN, a deep learning-based algorithm for the automatic determination of intracellular parasite burden from fluorescence microscopy images. *Med Image Anal* 2024; **91**: 103036. <https://doi.org/10.1016/j.media.2023.103036>
- 39** Gomes-Alves AG, Maia AF, Cruz T *et al.* Development of an automated image analysis protocol for quantification of intracellular forms of

- Leishmania* spp. *PLoS ONE* 2018; **13**: e0201747. <https://doi.org/10.1371/journal.pone.0201747>
- 40** Santarém N, Tavares J, Cordeiro-da-Silva A. *In vitro* infections of macrophage-like cell lines with *Leishmania infantum* for drug screening. *Methods Mol Biol* 2019; **1971**: 265–77. [https://doi.org/10.1007/978-1-4939-9210-2\\_14](https://doi.org/10.1007/978-1-4939-9210-2_14)
- 41** Fonseca-Berzal C, Arán VJ, Escario JA *et al.* Experimental models in Chagas disease: a review of the methodologies applied for screening compounds against *Trypanosoma cruzi*. *Parasitol Res* 2018; **117**: 3367–80. <https://doi.org/10.1007/s00436-018-6084-3>
- 42** Trindade JDAS, Freire-de-Lima CG, Côrte-Real S *et al.* Drug repurposing for Chagas disease: *in vitro* assessment of nimesulide against *Trypanosoma cruzi* and insights on its mechanisms of action. *PLoS ONE* 2021; **16**: e0258292. <https://doi.org/10.1371/journal.pone.0258292>
- 43** Caljon G, De Muylder G, Durnez L *et al.* Alice in microbes' land: adaptations and counter-adaptations of vector-borne parasitic protozoa and their hosts. *FEMS Microbiol Rev* 2016; **40**: 664–85. <https://doi.org/10.1093/femsre/fuw018>
- 44** Cantizani J, Gamallo P, Cotillo I *et al.* Rate-of-Kill (RoK) assays to triage large compound sets for Chagas disease drug discovery: application to GSK Chagas Box. *PLoS Negl Trop Dis* 2021; **15**: e0009602. <https://doi.org/10.1371/journal.pntd.0009602>
- 45** Wenzler T, Yang S, Braissant O *et al.* Pharmacokinetics, *Trypanosoma brucei gambiense* efficacy, and time of drug action of DB829, a preclinical candidate for treatment of second-stage human African trypanosomiasis. *Antimicrob Agents Chemother* 2013; **57**: 5330–43. <https://doi.org/10.1128/AAC.00398-13>
- 46** Bruhn DF, Wyllie S, Rodríguez-Cortés A *et al.* Pentacyclic nitrofurans that rapidly kill nifurtimox-resistant trypanosomes. *J Antimicrob Chemother* 2016; **71**: 956–63. <https://doi.org/10.1093/jac/dkv417>
- 47** Maes L, Beyers J, Mondelaers A *et al.* *In vitro* 'time-to-kill' assay to assess the cidal activity dynamics of current reference drugs against *Leishmania donovani* and *Leishmania infantum*. *J Antimicrob Chemother* 2017; **72**: 428–30. <https://doi.org/10.1093/jac/dkw409>
- 48** Van den Kerkhof M, Mabile D, Chatelain E *et al.* *In vitro* and *in vivo* pharmacodynamics of three novel antileishmanial lead series. *Int J Parasitol Drugs Drug Resist* 2018; **8**: 81–6. <https://doi.org/10.1016/j.ijpddr.2018.01.006>
- 49** van der Ende J, Schallig H. *Leishmania* animal models used in drug discovery: a systematic review. *Animals* 2023; **13**: 1650. <https://doi.org/10.3390/ani13101650>
- 50** Percie du Sert N, Hurst V, Ahluwalia A *et al.* The ARRIVE guidelines 2.0: updated guidelines for reporting animal research. *PLoS Biol* 2020; **18**: e3000410. <https://doi.org/10.1371/journal.pbio.3000410>
- 51** Nguyen HTT, Radwanska M, Magez S. Tipping the balance between erythroid cell differentiation and induction of anemia in response to the inflammatory pathology associated with chronic trypanosome infections. *Front Immunol* 2022; **13**: 1051647. <https://doi.org/10.3389/fimmu.2022.1051647>
- 52** Antoine-Moussiaux N, Magez S, Desmecht D. Contributions of experimental mouse models to the understanding of African trypanosomiasis. *Trends Parasitol* 2008; **24**: 411–8. <https://doi.org/10.1016/j.pt.2008.05.010>
- 53** Ndungu K, Thungu D, Wamwiri F *et al.* Route of inoculation influences *Trypanosoma congolense* and *Trypanosoma brucei brucei* virulence in Swiss white mice. *PLoS ONE* 2019; **14**: e0218441. <https://doi.org/10.1371/journal.pone.0218441>
- 54** Hulpia F, Mabile D, Campagnaro GD *et al.* Combining tubercidin and cordycepin scaffolds results in highly active candidates to treat late-stage sleeping sickness. *Nat Commun* 2019; **10**: 5564. <https://doi.org/10.1038/s41467-019-13522-6>
- 55** Hirumi H, Hirumi K, Doyle JJ *et al.* *In vitro* cloning of animal-infective bloodstream forms of *Trypanosoma brucei*. *Parasitology* 1980; **80**: 371–82. <https://doi.org/10.1017/S003118200000822>
- 56** Pomel S, Biot C, Bories C *et al.* Antiprotozoal activity of ferroquine. *Parasitol Res* 2013; **112**: 665–9. <https://doi.org/10.1007/s00436-012-3183-4>
- 57** Graca NA, Gaspar L, Costa DM *et al.* Activity of bisnaphthalimidopropyl derivatives against *Trypanosoma brucei*. *Antimicrob Agents Chemother* 2016; **60**: 2532–6. <https://doi.org/10.1128/AAC.02490-15>
- 58** Reuner B, Vassella E, Yutzy B *et al.* Cell density triggers slender to stumpy differentiation of *Trypanosoma brucei* bloodstream forms in culture. *Mol Biochem Parasitol* 1997; **90**: 269–80. [https://doi.org/10.1016/S0166-6851\(97\)00160-6](https://doi.org/10.1016/S0166-6851(97)00160-6)
- 59** McLatchie AP, Burrell-Saward H, Myburgh E *et al.* Highly sensitive *in vivo* imaging of *Trypanosoma brucei* expressing "red-shifted" luciferase. *PLoS Negl Trop Dis* 2013; **7**: e2571. <https://doi.org/10.1371/journal.pntd.0002571>
- 60** Jacobs RT, Nare B, Wring SA *et al.* SCYX-7158, an orally-active benzoxaborole for the treatment of stage 2 human African trypanosomiasis. *PLoS Negl Trop Dis* 2011; **5**: e1151. <https://doi.org/10.1371/journal.pntd.0001151>
- 61** González-Andrade P, Camara M, Ilboudo H *et al.* Diagnosis of trypanosomatid infections: targeting the spliced leader RNA. *J Mol Diagn* 2014; **16**: 400–4. <https://doi.org/10.1016/j.jmoldx.2014.02.006>
- 62** Jones EM, Colley DG, Tostes S *et al.* Amplification of a *Trypanosoma cruzi* DNA sequence from inflammatory lesions in human Chagasic cardiomyopathy. *Am J Trop Med Hyg* 1993; **48**: 348–57. <https://doi.org/10.4269/ajtmh.1993.48.348>
- 63** Benvenuti LA, Rogério A, Cavalcanti MM *et al.* An autopsy-based study of *Trypanosoma cruzi* persistence in organs of chronic chagasic patients and its relevance for transplantation. *Transpl Infect Dis* 2017; **19**: e12783. <https://doi.org/10.1111/tid.12783>
- 64** Ferreira AV, Segatto M, Menezes Z *et al.* Evidence for *Trypanosoma cruzi* in adipose tissue in human chronic Chagas disease. *Microbes Infect* 2011; **13**: 1002–5. <https://doi.org/10.1016/j.micinf.2011.06.002>
- 65** Chatelain E, Scandale I. Animal models of Chagas disease and their translational value to drug development. *Expert Opin Drug Discov* 2020; **15**: 1381–402. <https://doi.org/10.1080/17460441.2020.1806233>
- 66** Martín-Escolano R, Cebrían R, Maqueda M *et al.* Assessing the effectiveness of AS-48 in experimental mice models of Chagas' disease. *J Antimicrob Chemother* 2020; **75**: 1537–45. <https://doi.org/10.1093/jac/dkaa030>
- 67** Guedes-da-Silva FH, Batista DG, Silva D *et al.* Antitrypanosomal activity of sterol 14 $\alpha$ -demethylase (CYP51) inhibitors VNI and VFV in the Swiss mouse models of Chagas disease induced by the *Trypanosoma cruzi* Y strain. *Antimicrob Agents Chemother* 2017; **61**: e02098-16. <https://doi.org/10.1128/AAC.02098-16>
- 68** Soeiro MNC, Sales-Junior PA, Pereira VRA *et al.* Drug screening and development cascade for Chagas disease: an update of *in vitro* and *in vivo* experimental models. *Mem Inst Oswaldo Cruz* 2024; **119**: e240057. <https://doi.org/10.1590/0074-02760240057>
- 69** Planer JD, Hulverson MA, Arif JA *et al.* Synergy testing of FDA-approved drugs identifies potent drug combinations against *Trypanosoma cruzi*. *PLoS Negl Trop Dis* 2014; **8**: e2977. <https://doi.org/10.1371/journal.pntd.0002977>
- 70** Nagajothi F, Machado FS, Burleigh BA *et al.* Mechanisms of *Trypanosoma cruzi* persistence in Chagas disease. *Cell Microbiol* 2012; **14**: 634–43. <https://doi.org/10.1111/j.1462-5822.2012.01764.x>
- 71** Gabaldón-Figueira JC, Martínez-Peinado N, Escabia E *et al.* State-of-the-art in the drug discovery pathway for Chagas disease: a

- framework for drug development and target validation. *Res Rep Trop Med* 2023; **14**: 1–19. <https://doi.org/10.2147/RRTM.S415273>
- 72** Ayala EV, Rodrigues da Cunha G, Azevedo MA et al. C57BL/6  $\alpha$ -1,3-galactosyltransferase knockout mouse as an animal model for experimental Chagas disease. *ACS Infect Dis* 2020; **6**: 1807–15. <https://doi.org/10.1021/acinfecdis.0c00061>
- 73** Croft SL. Monitoring drug resistance in leishmaniasis. *TropMedIntHealth* 2001; **6**: 899–905. <https://doi.org/10.1046/j.1365-3156.2001.00754.x>
- 74** Croft SL, Sundar S, Fairlamb AH. Drug resistance in leishmaniasis. *ClinMicrobiolRev* 2006; **19**: 111–26. <https://doi.org/10.1128/CMR.19.1.111-126.2006>
- 75** Hendrickx S, Guerin PJ, Caljon G et al. Evaluating drug resistance in visceral leishmaniasis: the challenges. *Parasitology* 2018; **145**: 453–63. <https://doi.org/10.1017/S0031182016002031>
- 76** Sacks DL, Melby PC. Animal models for the analysis of immune responses to leishmaniasis. *Curr Protoc Immunol* 2001; **Chapter 19**: Unit 19.2. <https://doi.org/10.1002/0471142735.im1902s28>
- 77** Katakura K. An experimental challenge model of visceral leishmaniasis by *Leishmania donovani* promastigotes in mice. *Parasitol Int* 2016; **65**: 603–6. <https://doi.org/10.1016/j.parint.2016.03.008>
- 78** Olias-Molero AI, de la Fuente C, Cuquerella M et al. Antileishmanial drug discovery and development: time to reset the model? *Microorganisms* 2021; **9**: 2500. <https://doi.org/10.3390/microorganisms9122500>
- 79** Yardley V, Croft SL. Chapter 93—animal models of cutaneous leishmaniasis. In: Zak O, Sande MA, eds. *Handbook of Animal Models of Infection*. Academic Press, 1999; 775–81.
- 80** Pérez-Cabezas B, Cecilio P, Gaspar TB et al. Understanding resistance vs. susceptibility in visceral leishmaniasis using mouse models of *Leishmania infantum* infection. *Front Cell Infect Microbiol* 2019; **9**: 30. <https://doi.org/10.3389/fcimb.2019.00030>
- 81** Rodrigues V, Cordeiro-da-Silva A, Laforge M et al. Regulation of immunity during visceral *Leishmania* infection. *Parasit Vectors* 2016; **9**: 118. <https://doi.org/10.1186/s13071-016-1412-x>
- 82** Preham O, Pinho FA, Pinto AI et al. CD4(+) T cells Alter the stromal microenvironment and repress medullary erythropoiesis in murine visceral leishmaniasis. *Front Immunol* 2018; **9**: 2958. <https://doi.org/10.3389/fimmu.2018.02958>
- 83** Moore JW, Beattie L, Osman M et al. CD4+ recent thymic emigrants are recruited into granulomas during *Leishmania donovani* infection but have limited capacity for cytokine production. *PLoS ONE* 2016; **11**: e0163604. <https://doi.org/10.1371/journal.pone.0163604>
- 84** Melo GD, Goyard S, Lecoer H et al. New insights into experimental visceral leishmaniasis: real-time in vivo imaging of *Leishmania donovani* virulence. *PLoS Negl Trop Dis* 2017; **11**: e0005924. <https://doi.org/10.1371/journal.pntd.0005924>
- 85** Squires KE, Kirsch M, Silverstein SC et al. Defect in the tissue cellular immune response: experimental visceral leishmaniasis in euthymic C57BL/6 ep/ep mice. *Infect Immun* 1990; **58**: 3893–8. <https://doi.org/10.1128/iai.58.12.3893-3898.1990>
- 86** Loeuillet C, Bañuls AL, Hide M. Study of *Leishmania* pathogenesis in mice: experimental considerations. *Parasit Vectors* 2016; **9**: 144. <https://doi.org/10.1186/s13071-016-1413-9>
- 87** Engwerda CR, Ato M, Kaye PM. Macrophages, pathology and parasite persistence in experimental visceral leishmaniasis. *Trends Parasitol* 2004; **20**: 524–30. <https://doi.org/10.1016/j.pt.2004.08.009>
- 88** Mesquita I, Ferreira C, Barbosa AM et al. The impact of IL-10 dynamic modulation on host immune response against visceral leishmaniasis. *Cytokine* 2018; **112**: 16–20. <https://doi.org/10.1016/j.cyto.2018.07.001>
- 89** Eberhardt E, Bulte D, Van Bockstal L et al. Miltefosine enhances the fitness of a non-virulent drug-resistant *Leishmania infantum* strain. *J Antimicrob Chemother* 2019; **74**: 395–406. <https://doi.org/10.1093/jac/dky450>
- 90** Álvarez-Velilla R, Gutiérrez-Corbo MDC, Punzón C et al. A chronic bioluminescent model of experimental visceral leishmaniasis for accelerating drug discovery. *PLoS Negl Trop Dis* 2019; **13**: e0007133. <https://doi.org/10.1371/journal.pntd.0007133>
- 91** Melby PC, Chandrasekar B, Zhao W et al. The hamster as a model of human visceral leishmaniasis: progressive disease and impaired generation of nitric oxide in the face of a prominent Th1-like cytokine response. *J Immunol* 2001; **166**: 1912–20. <https://doi.org/10.4049/jimmunol.166.3.1912>
- 92** Loria-Cervera EN. Animal models for the study of leishmaniasis. *Rev Inst Med Trop Sao Paulo* 2014; **56**: 1–11. <https://doi.org/10.1590/S0036-46652014000100001>
- 93** Ong HB, Clare S, Roberts AJ et al. Establishment, optimisation and quantitation of a bioluminescent murine infection model of visceral leishmaniasis for systematic vaccine screening. *Sci Rep* 2020; **10**: 4689. <https://doi.org/10.1038/s41598-020-61662-3>
- 94** Jiménez-Antón MD, Grau M, Corral MJ et al. Efficient infection of hamster with *Leishmania donovani* by retro-orbital inoculation. *Virulence* 2019; **10**: 711–8. <https://doi.org/10.1080/21505594.2019.1649587>
- 95** Eberhardt E, Van den Kerkhof M, Bulte D et al. Evaluation of a pan-*Leishmania* spliced-leader RNA detection method in human blood and experimentally infected Syrian golden hamsters. *J Mol Diagn* 2018; **20**: 253–63. <https://doi.org/10.1016/j.jmoldx.2017.12.003>
- 96** Hendrickx R, Melkamu R, Tadesse D et al. Spliced-leader RNA as a dynamic marker for monitoring viable *Leishmania* parasites during and after treatment. *J Infect Dis* 2024; **230**: 183–7. <https://doi.org/10.1093/infdis/jiae219>
- 97** Sacks D, Noben-Trauth N. The immunology of susceptibility and resistance to *Leishmania major* in mice. *Nat Rev Immunol* 2002; **2**: 845–58. <https://doi.org/10.1038/nri933>
- 98** Rodrigues V, Cordeiro-da-Silva A, Laforge M et al. Impairment of T cell function in parasitic infections. *PLoS Negl Trop Dis* 2014; **8**: e2567. <https://doi.org/10.1371/journal.pntd.0002567>
- 99** Alexander J. Sex differences and cross-immunity in DBA/2 mice infected with *L. mexicana* and *L. major*. *Parasitology* 1988; **96**(Pt 2): 297–302. <https://doi.org/10.1017/S0031182000058303>
- 100** da Silva R, Sacks DL. Metacyclogenesis is a major determinant of *Leishmania* promastigote virulence and attenuation. *Infect Immun* 1987; **55**: 2802–6. <https://doi.org/10.1128/iai.55.11.2802-2806.1987>
- 101** Späth GF, Beverley SM. A lipophosphoglycan-independent method for isolation of infective *Leishmania* metacyclic promastigotes by density gradient centrifugation. *Exp Parasitol* 2001; **99**: 97–103. <https://doi.org/10.1006/expr.2001.4656>
- 102** Sacks DL, Hienny S, Sher A. Identification of cell surface carbohydrate and antigenic changes between noninfective and infective developmental stages of *Leishmania major* promastigotes. *J Immunol* 1985; **135**: 564–9. <https://doi.org/10.4049/jimmunol.135.1.564>
- 103** Lang T, Courret N, Colle JH et al. The levels and patterns of cytokines produced by CD4T lymphocytes of BALB/c mice infected with *Leishmania major* by inoculation into the ear dermis depend on the infectiousness and size of the inoculum. *Infect Immun* 2003; **71**: 2674–83. <https://doi.org/10.1128/IAI.71.5.2674-2683.2003>
- 104** Giraud E, Martin O, Yakob L et al. Quantifying *Leishmania* metacyclic promastigotes from individual sandfly bites reveals the efficiency of vector transmission. *Commun Biol* 2019; **2**: 84. <https://doi.org/10.1038/s42003-019-0323-8>
- 105** Kimblin N, Peters N, Debrabant A et al. Quantification of the infectious dose of *Leishmania major* transmitted to the skin by single sand flies. *Proc Natl Acad Sci U S A* 2008; **105**: 10125–30. <https://doi.org/10.1073/pnas.0802331105>

- 106** Van Bocxlaer K, Caridha D, Black C *et al.* Novel benzoxaborole, nitroimidazole and aminopyrazoles with activity against experimental cutaneous leishmaniasis. *Int J Parasitol Drugs Drug Resist* 2019; **11**: 129–38. <https://doi.org/10.1016/j.ijpddr.2019.02.002>
- 107** Caridha D, Vesely B, van Bocxlaer K *et al.* Route map for the discovery and pre-clinical development of new drugs and treatments for cutaneous leishmaniasis. *Int J Parasitol Drugs Drug Resist* 2019; **11**: 106–17. <https://doi.org/10.1016/j.ijpddr.2019.06.003>
- 108** Bretscher PA, Wei G, Menon JN *et al.* Establishment of stable, cell-mediated immunity that makes “susceptible” mice resistant to *Leishmania major*. *Science* 1992; **257**: 539–42. <https://doi.org/10.1126/science.1636090>
- 109** Lang T, Goyard S, Lebastard M *et al.* Bioluminescent *Leishmania* expressing luciferase for rapid and high throughput screening of drugs acting on amastigote-harboring macrophages and for quantitative real-time monitoring of parasitism features in living mice. *Cell Microbiol* 2005; **7**: 383–92. <https://doi.org/10.1111/j.1462-5822.2004.00468.x>
- 110** Constant SL, Lee KS, Bottomly K. Site of antigen delivery can influence T cell priming: pulmonary environment promotes preferential Th2-type differentiation. *Eur J Immunol* 2000; **30**: 840–7. [https://doi.org/10.1002/1521-4141\(200003\)30:3<840::AID-IMMU840>3.0.CO;2-L](https://doi.org/10.1002/1521-4141(200003)30:3<840::AID-IMMU840>3.0.CO;2-L)
- 111** Lewis MD, Fortes Francisco A, Taylor MC *et al.* Bioluminescence imaging of chronic *Trypanosoma cruzi* infections reveals tissue-specific parasite dynamics and heart disease in the absence of locally persistent infection. *Cell Microbiol* 2014; **16**: 1285–300. <https://doi.org/10.1111/cmi.12297>
- 112** Caljon G, Van Reet N, De Trez C *et al.* The dermis as a delivery site of *Trypanosoma brucei* for tsetse flies. *PLoS Pathog* 2016; **12**: e1005744. <https://doi.org/10.1371/journal.ppat.1005744>
- 113** Capewell P, Cren-Travaill e C, Marchesi F *et al.* The skin is a significant but overlooked anatomical reservoir for vector-borne African trypanosomes. *eLife* 2016; **5**: e17716. <https://doi.org/10.7554/eLife.17716>
- 114** De Niz M, Br as D, Ouarn e M *et al.* Organotypic endothelial adhesion molecules are key for *Trypanosoma brucei* tropism and virulence. *Cell Rep* 2021; **36**: 109741. <https://doi.org/10.1016/j.celrep.2021.109741>
- 115** Mabile D, Dirx L, Thys S *et al.* Impact of pulmonary African trypanosomes on the immunology and function of the lung. *Nat Commun* 2022; **13**: 7083. <https://doi.org/10.1038/s41467-022-34757-w>
- 116** Lewis MD, Francisco AF, Taylor MC *et al.* A new experimental model for assessing drug efficacy against *Trypanosoma cruzi* infection based on highly sensitive *in vivo* imaging. *J Biomol Screen* 2015; **20**: 36–43. <https://doi.org/10.1177/1087057114552623>
- 117** Hyland KV, Asfaw SH, Olson CL *et al.* Bioluminescent imaging of *Trypanosoma cruzi* infection. *Int J Parasitol* 2008; **38**: 1391–400. <https://doi.org/10.1016/j.ijpara.2008.04.002>
- 118** Andriani G, Chessler AD, Courtemanche G *et al.* Activity *in vivo* of anti-*Trypanosoma cruzi* compounds selected from a high throughput screening. *PLoS Negl Trop Dis* 2011; **5**: e1298. <https://doi.org/10.1371/journal.pntd.0001298>
- 119** Canavaci AM, Bustamante JM, Padilla AM *et al.* *In vitro* and *in vivo* high-throughput assays for the testing of anti-*Trypanosoma cruzi* compounds. *PLoS Negl Trop Dis* 2010; **4**: e740. <https://doi.org/10.1371/journal.pntd.0000740>
- 120** Francisco AF, Lewis MD, Jayawardhana S *et al.* Limited ability of posaconazole to cure both acute and chronic *Trypanosoma cruzi* infections revealed by highly sensitive *in vivo* imaging. *Antimicrob Agents Chemother* 2015; **59**: 4653–61. <https://doi.org/10.1128/AAC.00520-15>
- 121** Gonz alez S, Wall RJ, Thomas J *et al.* Short-course combination treatment for experimental chronic Chagas disease. *Sci Transl Med* 2023; **15**: eadg8105. <https://doi.org/10.1126/scitranslmed.adg8105>
- 122** Dominguez-Asenjo B, Guti errez-Corbo C, P erez-Pertejo Y *et al.* Bioluminescent imaging identifies thymus, as overlooked colonized organ, in a chronic model of *Leishmania donovani* mouse visceral leishmaniasis. *ACS Infect Dis* 2021; **7**: 871–83. <https://doi.org/10.1021/acscinfeddis.0c00864>
- 123** Rouault E, Lecoeur H, Meriem AB *et al.* Imaging visceral leishmaniasis in real time with golden hamster model: monitoring the parasite burden and hamster transcripts to further characterize the immunological responses of the host. *Parasitol Int* 2017; **66**: 933–9. <https://doi.org/10.1016/j.parint.2016.10.020>
- 124** Hendrickx S, Bult e D, Mabile D *et al.* Comparison of bioluminescent substrates in natural infection models of neglected parasitic diseases. *Int J Mol Sci* 2022; **23**: 16074. <https://doi.org/10.3390/ijms232416074>
- 125** Caridha D, Parriot S, Hudson TH *et al.* Use of optical imaging technology in the validation of a new, rapid, cost-effective drug screen as part of a tiered *in vivo* screening paradigm for development of drugs to treat cutaneous leishmaniasis. *Antimicrob Agents Chemother* 2017; **61**: e02048-16. <https://doi.org/10.1128/AAC.02048-16>
- 126** Dirx L, Hendrickx S, Merlot M *et al.* Long-term hematopoietic stem cells as a parasite niche during treatment failure in visceral leishmaniasis. *Commun Biol* 2022; **5**: 626. <https://doi.org/10.1038/s42003-022-03591-7>
- 127** Bogdan C, Islam NA, Barinberg D *et al.* The immunomicrotope of *Leishmania* control and persistence. *Trends Parasitol* 2024; **40**: 788–804. <https://doi.org/10.1016/j.pt.2024.07.013>
- 128** Dirx L, Van Acker SI, Nicolaes Y *et al.* Long-term hematopoietic stem cells trigger quiescence in *Leishmania* parasites. *PLoS Pathog* 2024; **20**: e1012181. <https://doi.org/10.1371/journal.ppat.1012181>
- 129** Brioschi MBC, Coser EM, Coelho AC *et al.* Models for cytotoxicity screening of antileishmanial drugs: what has been done so far? *Int J Antimicrob Agents* 2022; **60**: 106612. <https://doi.org/10.1016/j.ijantimicag.2022.106612>
- 130** Rajpoot K, Panchal M, Pawar B *et al.* Chapter 15—high-throughput screening in toxicity assessment. In: Tekade RK, ed. *Public Health and Toxicology Issues in Drug Research*. Academic Press, 2024; 407–49.
- 131** Andre S, Rodrigues V, Pemberton S *et al.* Antileishmanial drugs modulate IL-12 expression and inflammasome activation in primary human cells. *J Immunol* 2020; **204**: 1869–80. <https://doi.org/10.4049/jimmunol.1900590>
- 132** Cos P, Vlietinck AJ, Berghe DV *et al.* Anti-infective potential of natural products: how to develop a stronger *in vitro* ‘proof-of-concept’. *J Ethnopharmacol* 2006; **106**: 290–302. <https://doi.org/10.1016/j.jep.2006.04.003>
- 133** Mathiasen JR, Moser VC. The Irwin test and functional observational battery (FOB) for assessing the effects of compounds on behavior, physiology, and safety pharmacology in rodents. *Curr Protoc Pharmacol* 2018; **83**: e43. <https://doi.org/10.1002/cpph.43>
- 134** Kus M, Ibragimow I, Piotrowska-Kempisty H. Caco-2 cell line standardization with pharmaceutical requirements and *in vitro* model suitability for permeability assays. *Pharmaceutics* 2023; **15**: 2523. <https://doi.org/10.3390/pharmaceutics15112523>
- 135** Chen S, Einspanier R, Schoen J. Transepithelial electrical resistance (TEER): a functional parameter to monitor the quality of oviduct epithelial cells cultured on filter supports. *Histochem Cell Biol* 2015; **144**: 509–15. <https://doi.org/10.1007/s00418-015-1351-1>
- 136** Pond SM, Tozer TN. First-pass elimination. Basic concepts and clinical consequences. *Clin Pharmacokinet* 1984; **9**: 1–25. <https://doi.org/10.2165/00003088-198409010-00001>
- 137** Doherty MM, Pang KS. First-pass effect: significance of the intestine for absorption and metabolism. *Drug Chem Toxicol* 1997; **20**: 329–44. <https://doi.org/10.3109/01480549709003891>

- 138** Sha C, Cuperlovic-Culf M, Hu T. SMILE: systems metabolomics using interpretable learning and evolution. *BMC Bioinform* 2021; **22**: 284. <https://doi.org/10.1186/s12859-021-04209-1>
- 139** Liu B, Chang J, Gordon WP et al. Snapshot PK: a rapid rodent *in vivo* preclinical screening approach. *Drug Discov Today* 2008; **13**: 360–7. <https://doi.org/10.1016/j.drudis.2007.10.014>
- 140** Parasuraman S, Raveendran R, Kesavan R. Blood sample collection in small laboratory animals. *J Pharmacol Pharmacother* 2010; **1**: 87–93. <https://doi.org/10.4103/0976-500X.72350>
- 141** Li C, Liu B, Chang J et al. A modern *in vivo* pharmacokinetic paradigm: combining snapshot, rapid and full PK approaches to optimize and expedite early drug discovery. *Drug Discov Today* 2013; **18**: 71–8. <https://doi.org/10.1016/j.drudis.2012.09.004>
- 142** Gad SC, Spainhour CB, Shoemake C et al. Tolerable levels of non-clinical vehicles and formulations used in studies by multiple routes in multiple species with notes on methods to improve utility. *Int J Toxicol* 2016; **35**: 95–178. <https://doi.org/10.1177/1091581815622442>
- 143** Baral TN, Magez S, Stijlemans B et al. Experimental therapy of African trypanosomiasis with a nanobody-conjugated human trypanolytic factor. *Nat Med* 2006; **12**: 580–4. <https://doi.org/10.1038/nm1395>
- 144** Myburgh E, Coles JA, Ritchie R et al. *In vivo* imaging of trypanosome-brain interactions and development of a rapid screening test for drugs against CNS stage trypanosomiasis. *PLoS Negl Trop Dis* 2013; **7**: e2384. <https://doi.org/10.1371/journal.pntd.0002384>
- 145** Janse van Rensburg HD, N'Da DD, Suganuma K. *In vitro* and *in vivo* trypanocidal efficacy of nitrofuryl- and nitrothienylazines. *ACS Omega* 2023; **8**: 43088–98. <https://doi.org/10.1021/acsomega.3c06508>
- 146** Gillingwater K, Kunz C, Braghiroli C et al. *In vitro*, *ex vivo*, and *in vivo* activities of diamidines against *Trypanosoma congolense* and *Trypanosoma vivax*. *Antimicrob Agents Chemother* 2017; **61**: e02356-16. <https://doi.org/10.1128/AAC.02356-16>
- 147** Gillingwater K, Kumar A, Anbazhagan M et al. *In vivo* investigations of selected diamidine compounds against *Trypanosoma evansi* using a mouse model. *Antimicrob Agents Chemother* 2009; **53**: 5074–9. <https://doi.org/10.1128/AAC.00422-09>
- 148** Kangethe RT, Winger EM, Settypalli TBK et al. Low dose gamma irradiation of *Trypanosoma evansi* parasites identifies molecular changes that occur to repair radiation damage and gene transcripts that may be involved in establishing disease in mice post-irradiation. *Front Immunol* 2022; **13**: 852091. <https://doi.org/10.3389/fimmu.2022.852091>
- 149** Mekonnen G, Mohammed EF, Kidane W et al. Isometamidium chloride and homidium chloride fail to cure mice infected with Ethiopian *Trypanosoma evansi* type A and B. *PLoS Negl Trop Dis* 2018; **12**: e0006790. <https://doi.org/10.1371/journal.pntd.0006790>
- 150** Birhanu H, Gebrehiwot T, Goddeeris BM et al. New *Trypanosoma evansi* type B isolates from Ethiopian dromedary camels. *PLoS Negl Trop Dis* 2016; **10**: e0004556. <https://doi.org/10.1371/journal.pntd.0004556>
- 151** Gillingwater K. *In vitro* and *in vivo* efficacy of diamidines against *Trypanosoma equiperdum* strains. *Parasitology* 2018; **145**: 953–60. <https://doi.org/10.1017/S0031182017002098>
- 152** Cuypers B, Van den Broeck F, Van Reet N et al. Genome-wide SNP analysis reveals distinct origins of *Trypanosoma evansi* and *Trypanosoma equiperdum*. *Genome Biol Evol* 2017; **9**: 1990–7. <https://doi.org/10.1093/gbe/evx102>
- 153** Gaspar L, Coron RP, KongThoo Lin P et al. Inhibitors of *Trypanosoma cruzi* Sir2 related protein 1 as potential drugs against Chagas disease. *PLoS Negl Trop Dis* 2018; **12**: e0006180. <https://doi.org/10.1371/journal.pntd.0006180>
- 154** Fortin A, Hendrickx S, Yardley V et al. Efficacy and tolerability of oleyl-phosphocholine (OIPC) in a laboratory model of visceral leishmaniasis. *J Antimicrob Chemother* 2012; **67**: 2707–12. <https://doi.org/10.1093/jac/dks273>
- 155** Jimenez-Anton MD, Garcia-Calvo E, Gutierrez C et al. Pharmacokinetics and disposition of miltefosine in healthy mice and hamsters experimentally infected with *Leishmania infantum*. *Eur J Pharm Sci* 2018; **121**: 281–6. <https://doi.org/10.1016/j.ejps.2018.06.002>
- 156** Wyllie S, Brand S, Thomas M et al. Preclinical candidate for the treatment of visceral leishmaniasis that acts through proteasome inhibition. *Proc Natl Acad Sci U S A* 2019; **116**: 9318–23. <https://doi.org/10.1073/pnas.1820175116>
- 157** Dominguez-Asenjo B, Gutiérrez-Corbo C, Álvarez-Bardón M et al. *Ex vivo* phenotypic screening of two small repurposing drug collections identifies nifuratel as a potential new treatment against visceral and cutaneous leishmaniasis. *ACS Infect Dis* 2021; **7**: 2390–401. <https://doi.org/10.1021/acsinfectdis.1c00139>
- 158** Zhu X, Pandharkar T, Werbovetz K. Identification of new antileishmanial leads from hits obtained by high-throughput screening. *Antimicrob Agents Chemother* 2012; **56**: 1182–9. <https://doi.org/10.1128/AAC.05412-11>
- 159** Corman HN, Shoue DA, Norris-Mullins B et al. Development of a target-free high-throughput screening platform for the discovery of antileishmanial compounds. *Int J Antimicrob Agents* 2019; **54**: 496–501. <https://doi.org/10.1016/j.ijantimicag.2019.07.013>
- 160** Present C, Giroo RD, Lin C et al. N(6)-methyltuberacin gives sterile cure in a cutaneous *Leishmania amazonensis* mouse model. *Parasitology* 2024; **151**: 506–13. <https://doi.org/10.1017/S0031182024000362>
- 161** Pratti JE, Ramos TD, Pereira JC et al. Efficacy of intranasal LaAg vaccine against *Leishmania amazonensis* infection in partially resistant C57Bl/6 mice. *Parasit Vectors* 2016; **9**: 534. <https://doi.org/10.1186/s13071-016-1822-9>
- 162** Coelho AC, Oliveira JC, Espada CR et al. A luciferase-expressing *Leishmania braziliensis* line that leads to sustained skin lesions in BALB/c mice and allows monitoring of miltefosine treatment outcome. *PLoS Negl Trop Dis* 2016; **10**: e0004660. <https://doi.org/10.1371/journal.pntd.0004660>